IEEE Access
Multidisciplinary ⋮ Rapid Review ⋮ Open Access Journal

Received 11 May 2023, accepted 29 May 2023, date of publication 1 June 2023, date of current version 7 June 2023.

Digital Object Identifier 10.1109/ACCESS.2023.3281900

RESEARCH ARTICLE

Simulative Investigation of the Hybrid, Spatially Multiplexed MIMO-FSO Transmission System Under Atmospheric Turbulence

SHIVAJI SINHA[1], CHAKRESH KUMAR[1], AMMAR ARMGHAN[2], (Senior Member, IEEE), MEHTAB SINGH[3], MESHARI ALSHARARI[2], AND KHALED ALIQAB[2]

[1]University School of Information, Communication and Technology, Guru Gobind Singh Indraprastha University, New Delhi 110078, India
[2]Department of Electrical Engineering College of Engineering, Jouf University, Sakaka 72388, Saudi Arabia
[3]Department of Electronics and Communication Engineering, University Institute of Engineering, Chandigarh University, Mohali, Punjab 140413, India

Corresponding authors: Khaled Aliqab (kmaliqab@ju.edu.sa) and Chakresh Kumar (chakreshk@ipu.ac.in)

ABSTRACT An orbital angular momentum (OAM) technology, which uses twisted helical phase structure laser modes to carry multiplexed information, has shown excellent potential to improve the capacity of the free space optical communication (FSO) system under atmospheric turbulence (AT) conditions. A significant challenge in an OAM-based FSO transmission system is the optical signal power fading and induced crosstalk due to abrupt changes in atmospheric turbulence. This research paper, presents a design of a hybrid, spatially multiplexed MIMO-FSO transmission system that incorporates the features of 16-QAM, OAM, and OFDM techniques with spatial mode diversity (SMD) to achieve high transmission rates and channel capacity with reduced power penalty during mitigating the multipath fading effects in different turbulent atmospheric channel conditions. The simulation based results illustrate that the hybrid, spatially multiplexed MIMO-FSO system achieves superior BER performance for the transmission link of 2 km with a forward error correction (FEC) threshold limit of 3.8×10^{-3}. The Gamma-Gamma (GG) turbulent model is used to analyze the system performance under various atmospheric turbulence conditions in terms of the optical signal to noise ratio (OSNR), number of subcarriers, OAM states, channel capacity, and power penalty. Comparing with the OAM-multiplexed and OFDM-based FSO transmission system, the capacity performance of the proposed system is significantly improved, and the average improvement is obtained at 650% and 856.04% respectively, at 10 dB OSNR. Furthermore, the result clearly showing a 1.5 dB reduction in power penalty with an increase in transmitter lens aperture at a fixed lateral displacement (LD) of 1.5 mm. For large transmitter beam diameters, the power penalty analysis shows an increase in LD tolerance and a decrease in receiver angular error (RAE). A large numerical value of mode spacing leads to a higher-order OAM state, which leads to high power loss but less inter-channel crosstalk due to beam divergence.

INDEX TERMS Bit error rate (BER), channel capacity, orbital angular momentum (OAM) multiplexing, optical signal to noise ratio (OSNR), orthogonal frequency division multiplexing (OFDM)), power penalty (PP), quadrature amplitude modulation (QAM), spatial mode diversity (SMD).

I. INTRODUCTION

A number of multiplexing methods, including wavelength division multiplexing (WDM) [1], polarization division multiplexing (PDM) [2], and space division multiplexing (SDM) [3], have been used to increase the transmission capacity of a FSO communication system. However, due to the numerous limitations and complex FSO receiver architecture, implemented in the FSO system, it is difficult to substantially increase their transmission capacity further.

A new multiplexing technique, orbital angular momentum (OAM), has gained prominence among researchers to further increase the capacity of the FSO system by transmitting spatially orthogonal OAM multiplexed laser beams

The associate editor coordinating the review of this manuscript and approving it for publication was Sukhdev Roy.

over an atmospheric turbulent channel due to its unique properties [4]. OAM exploits the spatial helical structure of the twisted laser beam, which comprises an azimuthal phase term, $e^{j\varphi l}$ where l is the topological charge and φ is the azimuthal angle. An orthonormal basis is formed by an orthogonal, infinite, unbound OAM state. These orthogonal vortex beams have different OAM states, and can be used to carry spectral efficient and high-capacity simultaneous transmission of information from different users, each on a separate OAM channel [5]. There are different approaches to generating vortex beams, including spiral phase plates (SPP) such as phase holograms [6] and meta-surfaces [7] with hollow intensity distribution and a spiral phase front. Hence, OAM multiplexing can be assumed as a special case of space division multiplexing (SDM) to enhance the capacity of the FSO system. However, in addition to the numerous advantages, there are some significant drawbacks when OAM multiplexed signals propagate through a turbulent channel, which ultimately brings side effects on bit-error-rate (BER) performance at the detector end. Power penalty (PP), inter-modal, and intra-modal OAM channel crosstalk distort the helical phase fronts of the transmitted laser beam. Some complex approaches, such as adaptive optics compensation and digital signal processing (DSP), have been investigated in various research articles to minimize crosstalk [8]. The performance of the channel equalization has been analyzed on single carrier QPSK, BPSK, and NRZ modulated signals to mitigate the atmospherically induced crosstalk. Another challenge in OAM multiplexed signal transmission is maintaining the OAM states orthogonal as they propagate through the turbulence link due to signal diffraction [9]. As discussed in Kolmogorov's model, atmospheric turbulence is a continuous random process in which large air cells break into smaller cells due to local temperature variations. Consequently, the FSO channel becomes inhomogeneous due to the random distribution of the refractive index profile. During signal propagation, this mechanism results in the leaking of some electromagnetic energy from one OAM state to another OAM state [10].

In recent years, free-space optical communication systems based on OAM and OFDM techniques have been investigated by different researchers under different atmospheric scenario. Du and Wang [11] have experimentally demonstrated the use of Bessel beams to analyze the BER performance of the FSO link and to achieve a spectrum efficiency of 25.6 bit/s/Hz. References [12], [13] have also provided different perspectives on combining the OAM multiplexing technique with other existing multiplexing technologies to obtain a higher transmission rate and spectrum efficiency. To reduce problems caused by atmospheric turbulence, a DSP-based processing was presented in [14], whereas an adaptive optics-based strategy showed high-speed performance and an improvement in the FSO connection [15]. A MIMO least-mean-square (LMS) equalization-based technique has also been suggested to mitigate atmospheric turbulence in FSO communication [16]. A pilot-assisted least squares (LS) algorithm, has been discussed in [17] to mitigate the crosstalk and improve the efficiency of OAM-based FSO systems. References [18] and [19] have proposed a constant modulus algorithm and convolutional neural network (CNN) to improve the FSO communication system. Spatial-mode multiplexing (SMM), which is a substitute for mode-division multiplexing (MDM), has recently gained lots of attention for increasing the channel capacity of the FSO communication system using the MIMO concept [20].

This research paper investigates the performance of a high-speed, N-OAM state and 16-QAM modulated, hybrid, spatially multiplexed MIMO free-space optical communication model based on an adaptive MIMO approach using spatial mode diversity (SMD) under various atmospheric turbulence conditions. To increase the transmission channel capacity for the optimal set of OAM mode numbers, the effects of the MIMO-SMD scheme are investigated at the optical receiver end [15]. Furthermore, the OFDM technique is combined with N-state OAM channels to increase overall system capacity, minimize multipath fading, and maximize link distance in turbulent channels. The effect of N-optimal set of OAM-OFDM optical transmission links has rarely been analyzed for free space communication systems [21] by the researchers. In the proposed model, each OAM-OFDM channel carries 120 Gbps, 16-QAM data on a single wavelength of 1550 nm for a link distance of 2 km. Moreover, the link performance is investigated using the same optimal OAM set with different refractive index structure parameters, the number of OAM states, and the number of subcarriers. The power loss based on by beam divergence and various receiver lens aperture diameters is also examined for the proposed approach. The results illustrate that using different T_x-R_x receiver aperture diameter sizes, and choosing appropriate higher-order OAM modes, power loss in terms of power penalty can be minimized using the MIMO diversity scheme in the proposed system. The system robustness of the proposed system is also analyzed in terms of receiver angular error and lateral displacement between the transmitter and receiver.

The remaining section of this research paper is organized as follows: Section II discusses the simulation-based setup of the proposed hybrid spatially multiplexed MIMO-FSO model and its mathematical analysis in detail, whereas, channel capacity modelling using spatial mode diversity under the Gamma-Gamma (G-G) channel model are also discussed for different turbulence conditions. The mathematical calculations of the power penalty and the crosstalk model of the proposed system is explored in Section III. The numerical results and findings are discussed and reported in Section IV. Finally, the conclusion and future scope of this research work are summarized in Section V.

II. THE PROOSED SYSTEM MODEL DESIGN

The conceptual model of the traditional N-state, OAM mode multiplexed MIMO, free-space optical communication system is shown in Fig. 1, whereas the detailed structure of

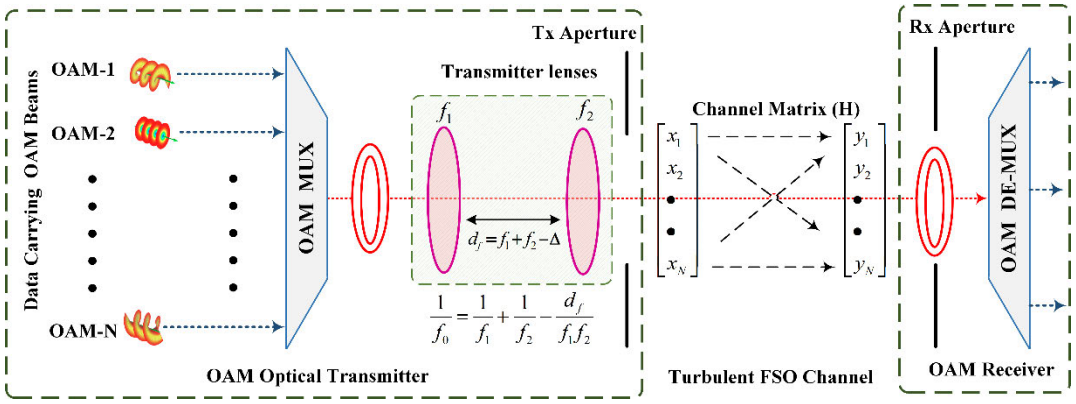

FIGURE 1. Principle of proposed hybrid spatially multiplexed MIMO-FSO transmission system.

the simulation-based system setup of the proposed hybrid spatially multiplexed MIMO, FSO communication system using OAM, OFDM and mode diversity scheme is illustrated in Fig. 2. The intended N-OAM and adjacent $N-1$ OAM modes with the same optical power, as shown in Fig. 1, form an independent and orthogonal OAM channel, each carrying a 120 Gbps data stream near an optical wavelength of $\lambda = 1550$ nm. These collimated OAM beams are further multiplexed using mode division multiplexing (MDM) in the OAM-MUX section. The spatially mode multiplexed (SMM) optical signal is then passed through a pair of lenses (with focal lengths of f_1 and f_2) having equivalent focal lengths of f_o and center-to-center lens spacing of d_f respectively. The multiplexed OAM signal is then focused towards the optical receiver by carefully selecting and adjusting the lens offset parameter Δ, and the proposed system design is made more robust against pointing errors by reducing power loss due to beam spreading [22]. This method can further help to minimize the T_x-R_x structure complexity by employing a spiral phase plate (SPP) technique to generate N state OAM modes. The transmit power for each mode is further scaled by $1/N$ to conserve the overall transmitted power by selecting appropriate mode spacing and T_x-R_x lens aperture sizes. This method is helpful in minimizing the power penalty (PP) of the proposed system design.

When the OAM multiplexed signal is transmitted over the atmospheric turbulence, the power coupling from one mode to adjacent modes may take place to create crosstalk and hence lead to signal fluctuations at the optical receiver end. So to mitigate this problem, the spatial mode diversity (SMD) scheme is introduced in our proposed system design to achieve minimum interruption probability with improved reliability of the FSO link.

The simulation-based-setup of the proposed hybrid, spatially multiplexed FSO system based on MIMO-spatial mode diversity scheme is illustrated in Fig. 2. An optical mode generator is used to split the Gaussian beam into N components where the i_{th} spatial multiplexed field for the Gaussian beam of ω_0 waist size and Lagrange Gaussian (LG) polynomial L_0^i is given by [23]

$$u_{i_{th}}(\omega_z, \varphi, 0) = \sqrt{\frac{2}{\pi\,|i|!}}\frac{1}{\omega_0}\left(\frac{\sqrt{2}\omega_z}{\omega_0}\right)^{|i|} L_0^i\left(\frac{2\omega_z^2}{\omega_0^2}\right) \times e^{-\left(\frac{\omega_z^2}{\omega_0^2}+ji\varphi\right)} \quad (1)$$

Then the signal $\bar{x_p}(t)$. $p = 1 \ldots\ldots\ldots N$, from each optical channel is loaded onto N-Gaussian beam through the intensity modulator (IM).

An arbitrary waveform generator, AWG 70001 operating at a sample rate of 40-G samples/s is used to generate a real valued 16-QAM encoded electrical discrete multi-tone (DMT) signal having effective bandwidth of 9.76 GHz. Using Hermitian symmetry, a real valued signal is generated for 512-point inverse fast Fourier transformation (IFFT) input. Then a cyclic prefix (CP) of 40 samples added DMT signal is further fed into IM modulator. The output from the N channel IM blocks is then fed to OFDM block. The n_{th} OFDM subcarrier frequency f_n for each channel is chosen from $f = \{f_o, f_2, \ldots\ldots f_n, \ldots, f_{n-1}\}$ given by Eq. (2) for symbol period T_s and minimum subcarrier frequency f_{sc}

$$f_n = \frac{n}{T_s} + f_{sc}, \quad 0 \le n \le M-1 \quad (2)$$

The mathematical equation of OAM-OFDM signal is represented by

$$S_{OAM-OFDM}(t) = \sum_{j=1}^{L}\sum_{u=0}^{U-1}\sum_{m=0}^{M-1} X_n^j e^{2\pi i f_{sc} t} e^{\frac{2\pi i u l_j}{U}} \quad (3)$$

This intensity modulated signal is further turned into vortex beam in a OAM state converter. OAM state converter is a spiral phase plate (SPP) which generates j_{th} OAM-OFDM states chosen from the set $S = \{-k, -k+1 \ldots 0 \ldots k, k+1\}$. Here, total $l = 2k+1$ OAM-OFDM states are generated in same frequency band assuming k as the maximum state. The matrix response from the OAM state multiplexer output

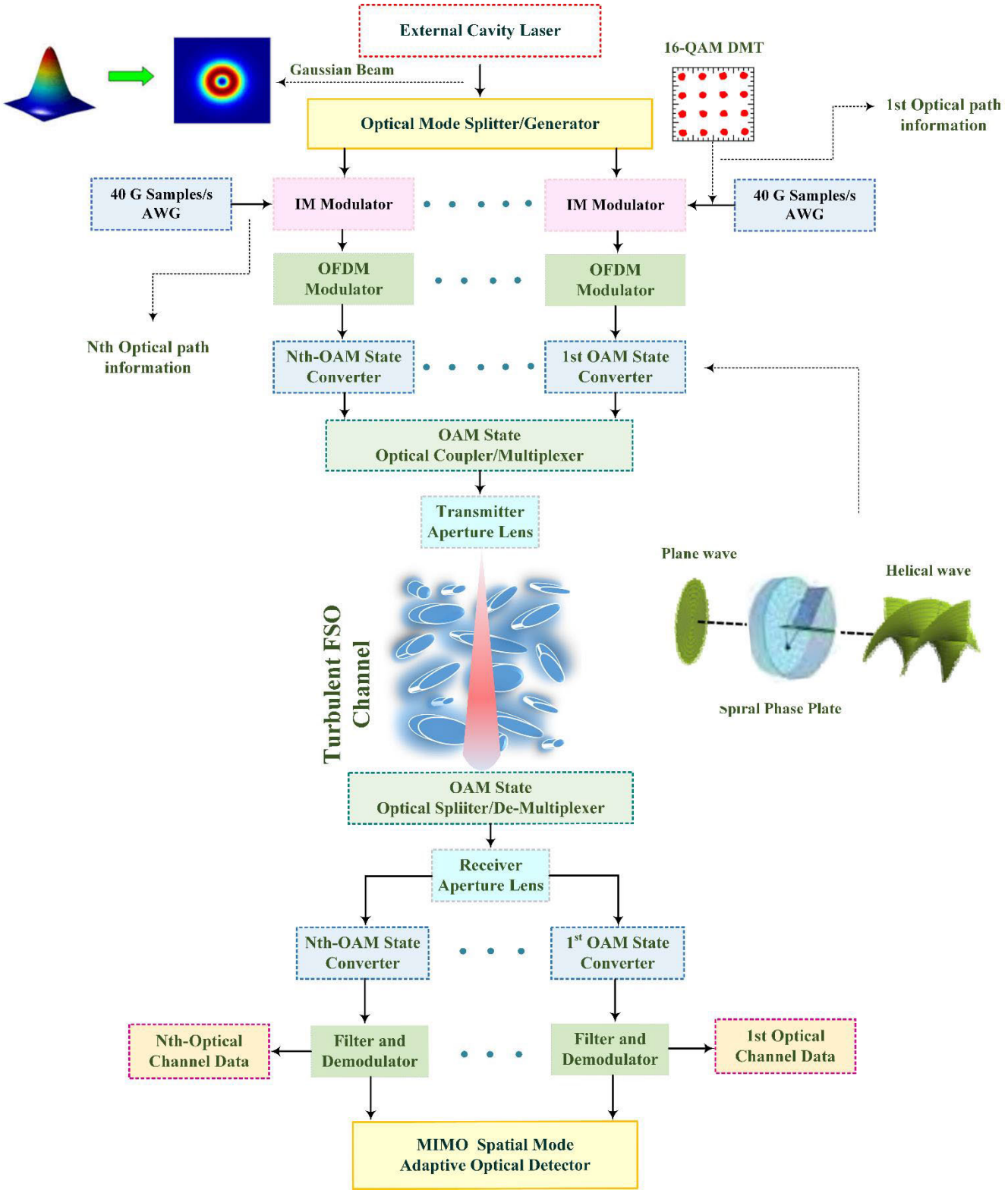

FIGURE 2. Simulation-based setup of the proposed hybrid, spatially multiplexed MIMO- FSO system.

is given by a matrix S [24]

$$S = [S_1(n), S_2(n) \ldots\ldots\ldots, S_N(n)]^T \tag{4}$$

The distorted signal matrix response at the output of the OAM de-multiplexer is shown by

$$\hat{S} = [\hat{S_1}(n), \hat{S_{21}}(n) \ldots\ldots\ldots, \hat{S_N}(n)]^T = HS \tag{5}$$

where H is a $N \times N$ atmospheric turbulence channel matrix for $h_{i,j}$, $1 \leq i, j \leq N$. The output from the OAM De-MUX is then demodulated and the output signal matrix from the demodulator and filter subsystem is expressed by

$$Y = [Y_1(n), Y_2(n), \ldots\ldots..Y_N(n)] = G\hat{S} \tag{6}$$

where G, is a mode multiplexed matrix for $g_{i,f}$, $1 \leq I, j \leq$ N.

The estimated SNR for the tap gain coefficient $W_{\ddot{y}}^{l}$ of length $L+1$ for the OAM-OFDM-MIMO spatial mode multiplexed signal is given as

$$\hat{y}_j(n) = \sum_{i=1}^{N}\sum_{l=0}^{L} w_{ij}^{l}\hat{s}_i(n-l) \tag{7}$$

III. CAPACITY MODELLING USING SPATIAL MODE DIVERSITY

The electric field distribution of the hybrid, MIMO spatial mode multiplexed signal [25] is given by

$$U_{Mux}(\omega_z, \phi, t) = \sum_{s=1}^{N} m_s(t)A_s(\omega_z)e^{il_s\phi} \tag{8}$$

where $m_s(t), A_s(\omega_z)$ and l_s are the 16-QAM modulated signal, field strength and quantum number respectively for distinctive angle mark 's'. The coherent coupling [26] in the optical light field is given by

$$S_{KNL}(r_k, \alpha_N, \phi_{L,}t) = \sqrt{r\alpha_N^2}e^{im\theta}e^{(-\theta)} + \sqrt{r(1-\alpha_N^2)} \times e^{-im\theta}e^{(\theta)} \tag{9}$$

where $r = r_k g(t)$, $\theta = e^{\left(-\frac{i\phi_L}{2}g(t)\right)}$.

In Eq. (9), r_k, and α_N are the total power in Gaussian beam $g(t)$, and power ratio between one beam and the total power. φ_{L} is the relative phase shift between two OAM beams respectively. The waist radius ω_z and the electric field [18] $\varphi(r, z)$ for the received OAM beam at a link distance of z can be given by

$$\omega_z = \omega_0\sqrt{(2\rho + l + 1)\left(1 + (\frac{\lambda z}{\pi\omega_0^2})\right)^2} \tag{10}$$

$$\phi(r, z) = \sum_{i=-\infty}^{+\infty}\sum_{k}\rho_k\alpha_{ki}u_i(r, z) \tag{11}$$

The received vector field $Y = [Y_1, Y_2 \ldots\ldots Y_N]^{\mathrm{T}}$, and corresponding received optical power in the $\mathrm{i_{th}}$ state of spatial mode diversity [23] is given by Eq. (12) and (13) respectively.

$$Y = |H_\rho|^2 \tag{12}$$

for N×N channel matrix H comprised of $\alpha_{i,j}$ and given by

$$H = \begin{bmatrix} \alpha_{11} & \cdot\cdot & \alpha_{N1} \\ \cdot & \cdot\cdot & \cdot \\ \alpha_{1N} & \cdot\cdot & \alpha N \end{bmatrix}$$
$$y_i = |\sum_{k}\rho_k\alpha_{ki}|^2 \tag{13}$$

where, α_{ki} is a link distance dependent complex value, and $\rho = [\rho_1, \rho_2, \ldots..\rho_N]^T$ is the transmitted signal vector respectively. Hence, the instantaneous asymptotic optical signal to noise ratio (OSNR) is also given by

$$\gamma_i = \frac{|\alpha_{ii}|^2}{\sum\limits_{k\in N, K\neq i} E[|\alpha_{ki}|^2]} \tag{14}$$

Turbulence-induced scintillation [18] is responsible for a random change in the atmospheric refractive index due to the local air pressure and temperature gradient and is a significant factor that affects the FSO link during signal propagation. This process also causes the leakage of transmitted signal power from one OAM mode to adjacent OAM modes, which results in modes overlapping with power penalties.

The intensity fluctuations in received multiplexed signal $I = x \times y$ for $x, y > 0$ are the product of large (α) and small (β) scale turbulent eddies. The probability density functions (pdf), which is governed by the GG distribution [18] can be written by Eq. (15)

$$f_x(x) = \frac{\alpha(\alpha x)^{\alpha-1}}{\Gamma\alpha}e^{-\alpha x}, \quad f_y(y) = \frac{\beta(\beta y)^{\beta-1}}{\Gamma\beta}e^{-\beta y} \tag{15}$$

$$\alpha = \left(\exp\left[\frac{0.49\sigma^2}{(1+1.11\sigma^{2.4})^{7/6}}\right] - 1\right)^{-1} > 0$$
$$\beta = \left(\exp\left[\frac{0.51\sigma^2}{(1+0.691\sigma^{2.4})^{5/6}}\right] - 1\right)^{-1} > 0 \tag{16}$$

The refractive structure parameter (Rytov constant), and propagation constant are represented by $\sigma^2 = 1.23C_n^2k^{7/6}z^{11/6}$ and k, respectively. To calculate the BER of the proposed system, refer Eq. (17)

$$\langle BER_{l,m}\rangle = \int_0^{\propto} 0.5f_I(I)erfc\sqrt{\frac{I^2\gamma_{l,m}}{2}}dI \tag{17}$$

Here, $f_I(I)$ is the PDF of the intensity fluctuation and $\gamma_{l,m}$ is the signal-to-interference ratio (SINR) of the proposed hybrid spatially multiplexed system due to phase fluctuations. So, the mean achievable rate (MAR) achieved at high transmitted power P_t, and the instantaneous asymptotic SNR γ_i are expressed by Eq. (18) and Eq. (19) respectively.

$$C_{i/\alpha_{ii}}^{\infty} = \frac{1}{2}\log(\frac{1}{2}\gamma_i + 2) - \frac{1}{2}\gamma_i - 1 + \frac{\sqrt{\gamma_i(\gamma_i+4)}}{2} - \sqrt{\frac{\pi}{4\gamma_I}} \tag{18}$$

$$\gamma_i = \frac{|\alpha_{ii}^{|2}}{\sum\limits_{k\in N, k\neq i} E[|\alpha_{ki}|^2]} \tag{19}$$

In our proposed system design, the transmitter aperture transmit hybrid spatially multiplexed channels, with each single channel carries 120 Gbps, 16-QAM modulated signal with error probability expressed by Eq. (20) where, N_0, and

$$P_e = 3Q\left(\sqrt{\frac{4E_{avg}}{5N_0}}\right)\left[1 - 0.75Q\sqrt{0.8\frac{E_{avg}}{5N_0}}\right] \tag{20}$$

$Q(\cdot)$ showing the noise power spectral density (PSD) and complementary error function [20], whereas the average signal-to-noise ratio (SNR) per bit by $\frac{E_{avg}}{N_0}$, respectively. Eq. (20) is referred to evaluate the performance of the proposed system in terms of minimum power transmitted per channel to achieve BER threshold of 3.8×10^{-3} [27]. Here, it is assumed that each channel is transmitting an equal amount of power with inter-channel crosstalk that is comparable to the noise at our defined BER threshold. The received signal power penalty is calculated referring Eq. (21), assuming $\alpha_{rj,m}$ as large and $\beta_{rj.m}$ as the small-scale eddy, respectively,

$$P_{penalty} = 10log_{10}\left(\frac{P_{rj,m}}{P_{r,m}}\right) dB$$
$$P_{rj,m} = P_{rq}\left(\alpha_{rj,m} - \beta_{rj,m}\frac{p_{r,j}}{N_o}\right)^{-1} \quad (21)$$

In Eq. (21), $P_{rj;m}$ represents the m_{th} channel minimum power required at the transmitter as described earlier in [26].

In subsequent section, the performance of the proposed system is discussed in terms of BER, channel capacity, number of different subcarriers, Number of OAM modes and power penalty under different atmospheric turbulence conditions represented by various refractive index structures parameters

IV. NUMERICAL RESULTS AND DISCUSSIONS

The Gaussian OAM beam produced by the laser source in proposed hybrid spatial multiplexed MIMO-FSO transmitted end has a waist size of $\omega_o = 0.02$ m with a wavelength of $\lambda = 1550$ nm. Total OAM mode states taken are 20 with each single OAM channel is carrying 120 Gbps, 16-QAM modulated data with the maximum propagation distance of 2 km considering the additive white Gaussian (AWGN) noise model and the BER threshold is set to at 3.8×10^{-3}. The total number of OFDM subcarrier chosen is 8 with minimum subcarrier frequency of 30 GHz and OFDM subcarrier interval of 1 kHz, whereas the calculated SNR is 10 dB. The optical signal is transmitted through the GG channel model [18] considering four different atmospheric turbulence channel conditions from weak to strong and represented by the refractive index structure parameters (RIS) ($C_n^2 = 6 \times 10^{-11}$, 4×10^{-11}, 2×10^{-11}, 4×10^{-12}) $m^{-2/3}$. Rest of the physical parameters used for the calculation in our proposed system and implemented in [28] are summarized and compared in Table 1.

Fig. 3, shows the performance of the proposed system using performance metrics BER with respect to the number of OAM states under different minimum subcarrier frequencies from 30 GHz to 120 GHz in atmospheric turbulence conditions. For the fixed OAM state, let us suppose for $l = 0$, the BER increases from 2.2×10^{-3} having RIS constant value of $C_n^2 = 6 \times 10^{-11}\ m^{-2/3}$ to 8.3×10^{-2} for RIS constant value of $4 \times 10^{-12}\ m^{-2/3}$ as the minimum subcarrier frequency increases from 30 GHz to 120 GHz respectively. This result clearly predicts that the signal with the highest minimum

TABLE 1. System simulation parameters.

Parameters	Proposed system values	Values in [28]
Transmitted power	-15 dBm	-5 dBm
Wavelength	1550 nm	1550 nm
Bit rate/channel	120 Gbps	20 Gbps
OAM states	20	4
Modulation scheme	16-QAM	QPSK
IFFT/FFT points	64	NA
Cyclic Prefix length	40	NA
OFDM symbols/frame	96	NA
Pilot symbols/frame	04	NA
Aperture focal length	0.5 m	0.5 m
Optical beam size	0.02 m	0.08 m
Maximum link range	3 Km.	0.2 Km
Photo-detector responsivity	1 A/W	0.9 A/W
Detector dark current	10 nA	10 nA
Thermal noise power density	10^{-22} W/Hz	10^{-22} W/Hz

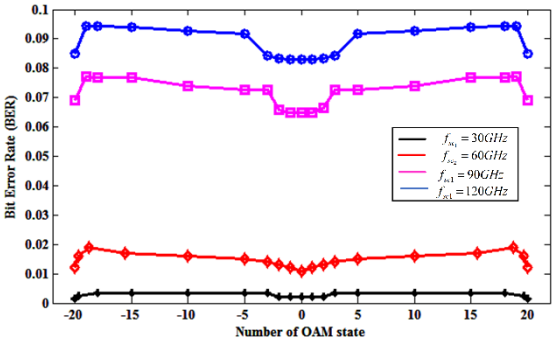

FIGURE 3. BER vs. OAM states for various minimum subcarrier frequencies.

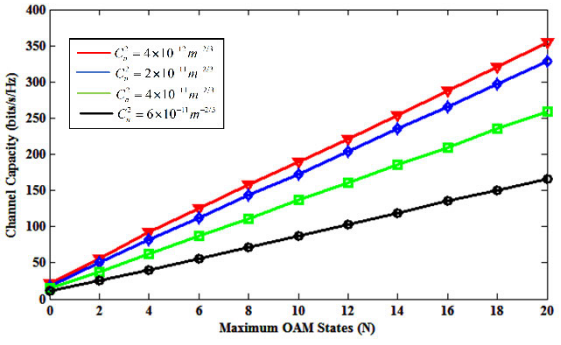

FIGURE 4. Channel capacity vs. maximum OAM state for various RIS constants.

subcarrier frequency under turbulence condition of RIS $4 \times 10^{-12}\ m^{-2/3}$ is the most sensitive and vulnerable with respect to the effect of the atmospheric turbulence, and resulting in higher BER. Hence, the proposed system performs best for 30 GHz sub carrier frequency and worst for 120 GHz subcarrier frequency, respectively.

The channel transmission capacity of the proposed hybrid spatially multiplexed MIMO-FSO system for different maximum OAM state under four refractive structure constants

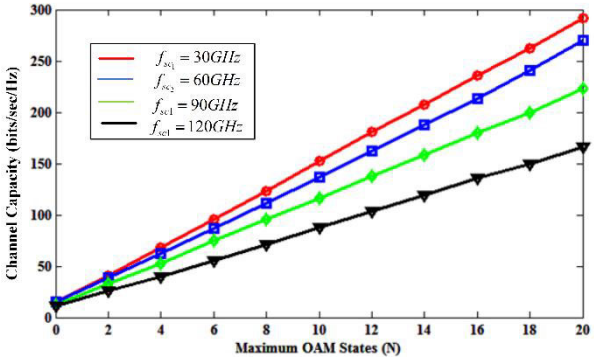

FIGURE 5. Channel capacity vs. maximum OAM state for different minimum subcarrier frequencies.

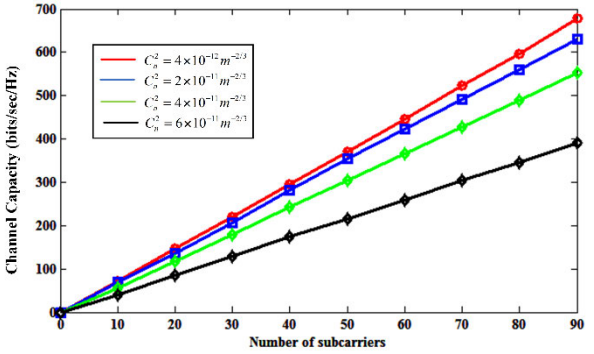

FIGURE 6. Capacity vs. number of subcarriers for different RIS.

which signify weak to strong atmospheric turbulence conditions are illustrated in Fig 4. By keeping fixed refractive index structure parameter say $C_n^2 = 6 \times 10^{-11}\ m^{-2/3}$ for black color curve, the capacity of the proposed FSO system increases from [11.3-166.7] bits/sec/Hz with the increase in number of OAM states from [0-20]. This result concludes that by increasing the number of OAM states, the number of OAM signals of different state to be multiplexed also increases and hence ultimately leads to enhancement in the capacity of the proposed hybrid spatially multiplexed MIMO-FSO system. On the other hand, if the OAM state is made constant, the transmission capacity of FSO system increases with the decrease in refractive index structure constant value in atmospheric turbulence. This result shows that the capacity of the proposed FSO system decreases with increase in BER and hence the increase in refractive index structure constant.

For minimum subcarrier frequencies under the different four types of atmospheric turbulence explained earlier, the increase in transmission channel capacity with respect to the increase in maximum OAM states is analyzed in Fig. 5. If the number of OAM states is kept constant, the capacity of the proposed FSO system increases with the decrease of the minimum subcarrier frequencies from 120 GHz to 30 GHz.

At OAM state $l = 6$, the capacity changes by 40.3 bits/sec/Hz for the change in minimum sub carrier frequencies from 120 GHz to 30 GHz, corresponding to weak to strong turbulence conditions. This shows that the BER performance decreases with the decrease in minimum subcarrier frequencies, which ultimately results in an increase in the system capacity of the proposed system.

Fig. 6, illustrates the enhancement of the transmission capacity of the proposed FSO transmission system, with respect to the increase in the number of subcarriers under four different RIS parameters corresponding from weak to strong atmospheric turbulence conditions. If the RIS parameter is made constant, the capacity of the proposed hybrid spatially multiplexed MIMO-FSO transmission system increases linearly with the increase in the number of subcarriers. This implies that increasing the number of OFDM subcarriers, which have to be multiplexed, will increase the capacity of the proposed transmission system. The graph also predicts that for a large number of OFDM subcarriers, the incremental change in channel capacity is also very large.

Fig. 7, demonstrates a performance comparison of the channel capacity with increasing OSNR values of the proposed hybrid spatially multiplexed MIMO-FSO system with the rest of the two FSO transmission systems under atmospheric turbulence conditions. The calculated channel capacities of the OFDM-FSO, OAM multiplexed FSO, and proposed hybrid spatially multiplexed MIMO-FSO systems are 9.10 bits/s/Hz, 11.6 bits/s/Hz, and 87 bits/s/Hz, respectively, at a fixed value of 10 dB OSNR. At a fixed value of 10 dB OSNR, the proposed system has a channel capacity improvement of 650% when compared to the OAM-based MIMO-FSO system, whereas the proposed system seems to have a significant enhancement of 856.04% when compared to the OFDM-based MIMO-FSO transmission system, as calculated in Eq (22).

$$\left(\frac{87-11.6}{11.6}\right) \times 100 = 650\%$$
$$\left(\frac{87-9.1}{9.1}\right) \times 100 = 856.04\% \qquad (22)$$

There is hardly any noticeable channel capacity gain for the [−10 to −5] dB OSNR range, but above this range, the capacity of the proposed system improves exponentially until 10 dB and does not increase significantly beyond this limit. The proposed model's channel capacity should theoretically be eight times greater ($8 \times 11.6 = 92.8$) bits/s/Hz than the capacity of the OAM multiplexed FSO system. Because of the impact of atmospheric turbulence, practically the average channel capacity deviation of (92.8−87=5.8) bits/sec/Hz is observed as shown in Fig. (7).

The exponential enhancement of power penalty (PP) with respect to increasing in lateral displacement (LD) for the three different transmitted beam sizes of $D_{tx} = [4, 6, \text{and } 8]$ cm. and keeping the constant link distance of 2 km are shown in Fig 8. The graph clearly shows that the almost 3.15 dB PP is less suffered by the transmitted beam of size $D_{tx} = 8$ cm compared to the beam size of $D_{tx} = 4$ cm for the fixed lateral displacement of 1.5 mm. The maximum PP

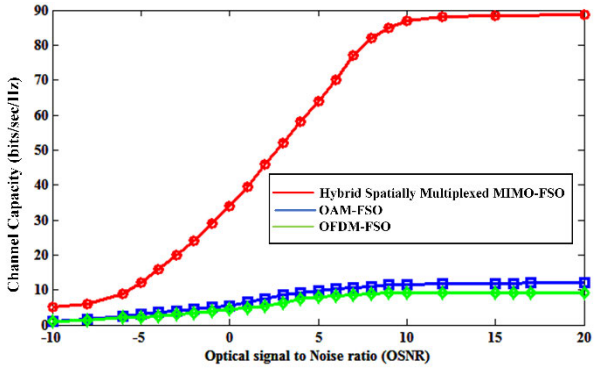

FIGURE 7. Channel capacity vs. OSNR for OAM, OFDM and proposed hybrid spatially multiplexed MIMO-FSO systems.

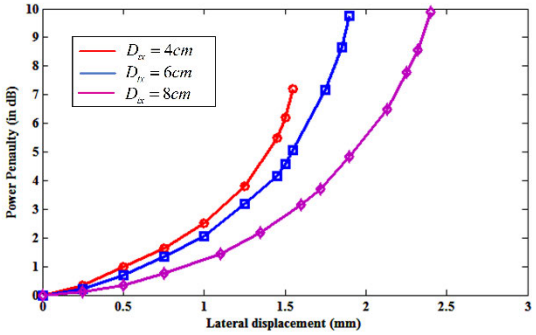

FIGURE 8. Comparison of power penalty vs. lateral displacement.

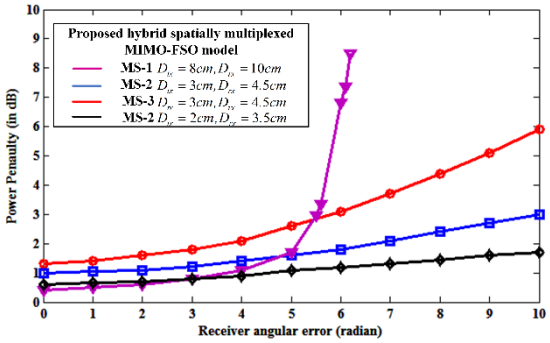

FIGURE 9. Comparison of power penalty vs. receiver angular error (RAE).

of 6.2 dB is suffered by $D_{tx} = 4$ cm beam size, whereas the minimum PP of 3.05 dB is suffered by the $D_{tx} = 8$ cm beam size at fixed LD = 1.5 mm, respectively. The result obtained from the graph also shows that with the increase in lateral displacement, these PPs increase more prominently. Also, if the lower transmitted beam size is made fixed, the power penalty is also minimal.

Fig. 9, demonstrates the power penalty result for the proposed hybrid spatially multiplexed MIMO-FSO system over a fixed link distance of 2 km for different transmitted and received beam sizes, respectively. For the mode spacing MS = 2, $D_{tx} = 3$ cm, and $D_{rx} = 4.5$ cm beam size, the proposed system offers better performance than MS = 1 when RAE ≥ 5 μrad. The obtained results also predict that the power penalty is slightly larger (0.63 dB) if we choose a T_x-R_x beam size of $D_{tx} = 8$ cm, $D_{rx} = 10$ cm compared to that of $D_{tx} = 3$ cm, $D_{rx} = 4.5$ cm, respectively [28]. The proposed system with MS = 2, $D_{tx} = 2$ cm, and $D_{rx} = 3.5$ cm. shows a lower PP of 0.53 dB. The PP analysis indicates that a large transmitted beam size and receiver aperture can increase the tolerance to LD but decrease the RAE. Also, if we select a large MS, the high OAM order results in higher signal power loss due to beam divergence; however, these systems offer less inter-channel crosstalk. If we keep MS = 1, $D_{tx} = 8$ cm, $D_{rx} = 10$ cm, the PP is higher than MS=2, $D_{tx} = 2$ cm, and $D_{rx} = 3.5$ cm for RAE. On comparing the results in Fig. 8 and in Fig. 5 in reference [20], they clearly demonstrate the reduced power penalty and inter-channel crosstalk.

V. CONCLUSION AND FUTURE WORK

In this study, we use OAM, OFDM, and MIMO/SMD multiplexed approaches to create a future high-speed and spectral-efficient free-space optical communication system with enhanced channel capacity, minimal power penalty, and crosstalk that takes atmospheric turbulence into account. The mathematical model for the BER model is also derived for the proposed system. Moreover, the obtained results demonstrate an almost 650% average capacity improvement over the OAM FSO transmission system for a link distance of 2 km. When we transmit the proposed system signal with MS = 2, over a link distance of 2 km, the power penalty of less than 1 dB is achieved. The results also demonstrate that the proposed hybrid spatially multiplexed MIMO-FSO transmission model achieves enhanced BER performance and channel capacity with the least amount of complexity under turbulent atmospheric conditions. In future work, an improved FSO system model can be developed by incorporating the FEC channel coding techniques with the existing proposed FSO system model to further enhance the BER and improve the channel capacity.

REFERENCES

[1] D. Sisodiya, S. Dwivedi, and G. Kaur, "Pol-SK based WDM-FSO communication system for network enhancement," in *Proc. IEEE 4th Int. Conf. Comput., Power Commun. Technol. (GUCON)*, Sep. 2021, pp. 1–5, doi: 10.1109/GUCON50781.2021.9573661.

[2] X. Zhou, J. Yu, M.-F. Huang, Y. Shao, T. Wang, L. Nelson, P. Magill, M. Birk, P. I. Borel, D. W. Peckham, R. Lingle, and B. Zhu, "64-Tb/s, 8 b/s/Hz, PDM-36QAM transmission over 320 km using both pre- and post-transmission digital signal processing," *J. Lightw. Technol.*, vol. 29, no. 4, pp. 571–577, Feb. 13, 2011, doi: 10.1109/JLT.2011.2105856.

[3] X. Liu, S. Chandrasekhar, X. Chen, P. J. Winzer, Y. Pan, T. F. Taunay, B. Zhu, M. Fishteyn, M. F. Yan, J. M. Fini, E. M. Monberg, and F. V. Dimarcello, "112-Tb/s 32-QAM-OFDM superchannel with 86-b/s/Hz intrachannel spectral efficiency and space-division multiplexed transmission with 60-b/s/Hz aggregate spectral efficiency," *Opt. Exp.*, vol. 19, no. 26, p. B958, 2011.

[4] A. M. Yao and M. J. Padgett, "Orbital angular momentum: Origins, behavior and applications," *Adv. Opt. Photon.*, vol. 3, no. 3, pp. 161–204, Jun. 2011, doi: 10.1364/AOP.3.000161.

[5] A. E. Willner and H. Song, "Optical angular momentum beams for high-capacity communications," *J. Lightw. Technol.*, vol. 41, no. 7, pp. 1–77, Apr. 1, 2023, doi: 10.1109/JLT.2022.3230585.

[6] N. Zhou, S. Zheng, X. Cao, Y. Zhao, S. Gao, Y. Zhu, M. He, X. Cai, and J. Wang, "Ultra-compact broadband polarization diversity orbital angular momentum generator with 3.6×3.6 μm^2 footprint," *Sci. Adv.*, vol. 5, no. 5, p. 9593, May 2019.

[7] J. Wang, "Metasurfaces enabling structured light manipulation," *Chin. Opt. Lett.*, vol. 16, Jan. 2018, Art. no. 050006.

[8] Y. Ren, G. Xie, H. Huang, L. Li, N. Ahmed, Y. Yan, and M. P. J. Lavery, "Turbulence compensation of an orbital angular momentum and polarization-multiplexed link using a data-carrying beacon on a separate wavelength," *Opt. Lett.*, vol. 40, no. 10, pp. 2249–2252, 2015, doi: 10.3788/COL201816.050006.

[9] H. Huang, Y. Cao, G. Xie, Y. Ren, Y. Yan, C. Bao, N. Ahmed, M. A. Neifeld, S. J. Dolinar, and A. E. Willner, "Crosstalk mitigation in a free-space orbital angular momentum multiplexed communication link using 4?4 MIMO equalization," *Opt. Lett.*, vol. 39, no. 15, pp. 4360–4363, 2014.

[10] Y. Ata, Y. Baykal, and M. C. Gökçe, "Average channel capacity in anisotropic atmospheric non-Kolmogorov turbulent medium," *Opt. Commun.*, vol. 451, pp. 129–135, Nov. 2019.

[11] J. Du and J. Wang, "High-dimensional structured light coding/decoding for free-space optical communications free of obstructions," *Opt. Lett.*, vol. 40, no. 21, pp. 4827–4830, 2015.

[12] J. W. Jian Wang, "Data information transfer using complex optical fields: A review and perspective," *Chin. Opt. Lett.*, vol. 15, no. 3, pp. 30005–30009, 2017.

[13] S. Li, S. Chen, C. Gao, A. E. Willner, and J. Wang, "Atmospheric turbulence compensation in orbital angular momentum communications: Advances and perspectives," *Opt. Commun.*, vol. 408, pp. 68–81, Feb. 2018.

[14] S. Chen, S. Li, Y. Zhao, J. Liu, L. Zhu, A. Wang, J. Du, Li Shen, and J. Wang, "Demonstration of 20-Gbit/s high-speed Bessel beam encoding/decoding link with adaptive turbulence compensation," *Opt. Lett.*, vol. 41, no. 20, pp. 4680–4683, 2016.

[15] S. Li and J. Wang, "Compensation of a distorted N-fold orbital angular momentum multicasting link using adaptive optics," *Opt. Lett.*, vol. 41, no. 7, pp. 1482–1485, Apr. 2016.

[16] L. Zou, L. Wang, C. Xing, J. Cui, and S. Zhao, "Turbulence mitigation with MIMO equalization for orbital angular momentum multiplexing communication," in *Proc. 8th Int. Conf. Wireless Commun. Signal Process. (WCSP)*, Oct. 2016, pp. 1–4.

[17] T. Sun, M. Liu, Z. Li, Y. Li, Q. Zhang, and M. Wang, "A crosstalk mitigation algorithm for OFDM-carrying OAM multiplexed FSO links," in *Proc. Opto-Electron. Commun. Conf. (OECC) Photon. Global Conf. (PGC)*, Jul. 2017, pp. 1–4.

[18] L. Wang, F. Jiang, M. Chen, H. Dou, G. Gui, and H. Sari, "Interference mitigation based on optimal modes selection strategy and CMA-MIMO equalization for OAM-MIMO communications," *IEEE Access*, vol. 6, pp. 69850–69859, 2018.

[19] J. Li, M. Zhang, D. Wang, S. Wu, and Y. Zhan, "Joint atmospheric turbulence detection and adaptive demodulation technique using the CNN for the OAM-FSO communication," *Opt. Exp.*, vol. 26, no. 8, pp. 10494–10508, 2018.

[20] B. B. Yousif, E. E. Elsayed, and M. M. Alzalabani, "Atmospheric turbulence mitigation using spatial mode multiplexing and modified pulse position modulation in hybrid RF/FSO orbital-angular-momentum multiplexed based on MIMO wireless communications system," *Opt. Commun.*, vol. 436, pp. 197–208, Apr. 2019.

[21] T. Hu, Y. Wang, L. Xi, J. Zhang, and Q. Song, "OFDM-OAM modulation for future wireless communications," *IEEE Access*, vol. 7, pp. 59114–59125, 2019.

[22] L. Li, G. Xie, Y. Ren, N. Ahmed, H. Huang, Z. Zhao, P. Liao, M. P. J. Lavery, Y. Yan, C. Bao, Z. Wang, A. J. Willner, N. Ashra, S. Ashra, M. Tur, and A. E. Willner, "Orbital-angular-momentum multiplexed free-space optical communication link using transmitter lenses," *Appl. Opt.*, vol. 55, no. 8, pp. 2098–2103, 2016.

[23] D. Lee, H. Sasaki, H. Fukumoto, Y. Yagi, T. Kaho, H. Shiba, and T. Shimizu, "An experimental demonstration of 28 GHz band wireless OAM-MIMO (orbital angular momentum multi-input and multi-output) multiplexing," in *Proc. IEEE 87th Veh. Technol. Conf.*, Porto, Portugal, Jun. 2018, pp. 1–5.

[24] Y. Li, K. Morgan, W. Li, J. K. Miller, R. Watkins, and E. G. Johnson, "Multi-dimensional QAM equivalent constellation using coherently coupled orbital angular momentum (OAM) modes in optical communication," *Opt. Exp.*, vol. 26, no. 23, pp. 30969–30977, 2018.

[25] S. Huang, G. R. Mehrpoor, and M. Safari, "Spatial-mode diversity and multiplexing for FSO communication with direct detection," *IEEE Trans. Commun.*, vol. 66, no. 5, pp. 2079–2092, May 2018, doi: 10.1109/TCOMM.2018.2795616.

[26] P. Kaur, V. K. Jain, and S. Kar, "Performance analysis of FSO array receivers in presence of atmospheric turbulence," *IEEE Photon. Technol. Lett.*, vol. 26, no. 12, pp. 1165–1168, Jun. 15, 2014.

[27] *Forward Error Correction for High Bit-Rate DWDM Submarine Systems*, document ITU-T G.975.1, 2004. [Online]. Available: https://www.itu.int/rec/T-REC-G.975.1-200402-I/en

[28] L. Zou, L. Wang, and S. Zhao, "Turbulence mitigation scheme based on spatial diversity in orbital-angular-momentum multiplexed system," *Opt. Commun.*, vol. 400, pp. 123–127, Oct. 2017.

SHIVAJI SINHA received the Bachelor of Engineering degree in electronics and communication engineering from Hemwati Nandan Bahuguna Central University, Uttarakhand, India, in 2003, and the Master of Technology degree in VLSI design from Dr. A. P. J. Abdul Kalam Technical University, India. He is currently pursuing the Ph.D. degree with Guru Gobind Singh Indraprastha University, New Delhi, India. He has 19 years of experience as a Faculty Member in academics. He is an Assistant Professor with the Department of Electronics and Communication Engineering, JSS Academy of Technical Education, Noida, India. He has published research papers in international journals and conferences. His research interests include electromagnetic field theory, antenna and wave propagation, mobile and wireless communication, and optical wireless communication. He is a member of various professional societies, such as IETE, ISTE, IEANG, and AMIE.

CHAKRESH KUMAR received the Ph.D. degree from I. K. Gujral, Punjab Technical University, Jalandhar. He is currently an Assistant Professor with USICT, Guru Gobind Singh Indraprastha University, New Delhi, India. Before taking the current assignment, he was an Assistant Professor with the Department of Electronics and Communication Engineering, Tezpur Central University Assam, India. He was also selected for the post of Assistant Professor with the Department of Electronics and Communication Engineering, Shri Mata Vaishno Devi University (SMVDU), Katra, Jammu and Kashmir, in 2012. He is an Alumnus of the Indian Institute of Technology (Indian School of Mines), Dhanbad. He has published more than 120 research articles in international journals, more than 130 research papers in international conferences, eight books with international publishers, and one patent under his credit. His research interests include high-speed optical communication systems and networks. He is a Life Time Member of ISTE, SSI, and IETE. He is serving as an Editor Board Member and an International Scientific Member of technical journals and societies in Prague, Czechia, Istanbul, Turkey, Paris, France, London, U.K., and many more. He received many prestigious awards, such as the Honor of the International Plato Award for Educational Achievement, the Bharat Jyoti Award, the Shiksha Rattan Puraskar from Dr. Bhishma Narain Singh Former Governor of Tamil Nadu and Assam, the Honor of the Bentham Ambassador for India, the Honor of the Young Scientist Award and Outstanding Scientist Award, in 2011, 2013, 2014, 2019, and 2020 respectively. He received the Certificate of Felicitation and the Honor of Rashtriya Gaurav and Bharat Excellence Award along with the Certificate of Outstanding Contribution in Teaching and Research from Dr. G. V. G. Krishnamurty Hon'ble Former Election Commissioner of India, in 2015. He received the Certificate of Appreciation from Texas Instruments for fostering an ecosystem bridging government, industry, and academia, in 2019. He has also been conferred the Faculty Achievement Award by Guru Gobind Singh Indraprastha University in recognition of his significant scholarly contribution to academic excellence in the field of professional education, in 2020.

AMMAR ARMGHAN (Senior Member, IEEE) received the bachelor's degree from COMSATS University, in 2006, the M.S. degree in electronics and communication engineering from the University of Nottingham, in 2010, and the Ph.D. degree from the Wuhan National Laboratory of Optoelectronic, Huazhong University of Science and Technology, Wuhan, China. He is currently an Assistant Professor of electrical engineering with Jouf University. He has published more than 70 high-impact factor articles in the last three years. His research interests include machine learning, complementary metamaterial-based microwave and terahertz devices, biosensors, optics, and photonics. He is a Reviewer of several reputed journals, such as IEEE Access, *CMC*, *Big Data*, *Sensors* (MDPI), *Applied Sciences* (MDPI), and *Electronics* (MDPI).

MEHTAB SINGH received the Bachelor of Engineering degree in electronics and communication engineering from the Thapar Institute of Engineering and Technology, Patiala, India, and the Master of Technology degree in electronics and communication engineering with specialization in communication systems and the Doctor of Philosophy degree in electronics technology from Guru Nanak Dev University, Amritsar, India. He has published over 80 research articles in SCI/SCIE and SCOPUS-indexed journals and conferences. His research interests include optical communication systems (wired and wireless), photonic radars, and opto-electronic devices. He serves as an Academic Editor for *International Journal of Optics* (Hindawi) and *Frontiers in Signal Processing*. He is featured in the World's Top 2% Scientist List released by Stanford University and Elsevier B. V., in October 2021 and 2022.

MESHARI ALSHARARI received the M.Sc. degree (Hons.) in mobile communications and the Ph.D. degree in electrical engineering from Heriot-Watt University, Edinburgh, U.K., in 2015 and 2021, respectively. He is currently an Assistant Professor with the Department of Electrical Engineering, Jouf University. His current research interests include the digital fabrication of soft and flexible electronics via a combination of advanced electronic materials and 3D printing technologies for applications in wireless communications, satellite, RF/microwave components, 3D printed sensors, and biomedical and health monitoring devices.

KHALED ALIQAB was born in Sakaka, Saudi Arabia, in 1990. He received the B.Eng. degree (Hons.) in electrical and electronic engineering, the M.Sc. degree (Hons.) in mobile communications, and the Ph.D. degree in electrical engineering from Heriot-Watt University, Edinburgh, U.K., in 2015 and 2021. He is currently an Assistant Professor with the Department of Electrical Engineering, Jouf University. His current research interests include advanced miniature multilayer self-packaged components, balanced differential circuit design, advanced radio frequency (RF)/microwave device technologies, liquid-crystal polymer (LCP) material, metamaterials, 3D printing, wireless communication radar and satellite applications, biomedical sensors and applications, and others.